25, 345 (1970).
[35]D. S. Greywall, Phys. Rev. A 3, 2106 (1971).
[36]J. F. Jarvis, D. Ramm, and H. Meyer, Phys. Rev. 170, 320 (1968).
[37]P. N. Henriksen, M. F. Panczyk, S. B. Trickey, and E. D. Adams, Phys. Rev. Letters 23, 518 (1969).
[38]G. Ahlers, Phys. Letters 22, 404 (1966).

PHYSICAL REVIEW A VOLUME 7, NUMBER 3 MARCH 1973

Neutron Scattering by Liquid Neon*

W. C. Kerr
Department of Physics, Wake Forest University, Winston-Salem, North Carolina 27109
Argonne National Laboratory, Argonne, Illinois 60439

K. S. Singwi
Department of Physics, Northwestern University, Evanston, Illinois 60201
Argonne National Laboratory, Argonne, Illinois 60439

(Received 1 September 1972)

A theory for neutron scattering by a semiclassical system, which is appropriate for liquid neon, is described. The theory is based on a generalized mean-field approximation involving the polarization potential and the screened response function, similarly to what has been done previously for argon and helium. The screened response function is assumed to be a sum of Gaussian functions weighted by the momentum-distribution function. The polarization potential and the width of the Gaussians are determined by the zeroth and third moments of the scattering law. The momentum distribution has the Maxwell–Boltzmann form, but includes quantum corrections to order $\hbar^2$. The quantum-mechanical zero-point energy is found to increase the kinetic energy per particle to a value of about 30% greater than the classical equipartition value. Calculations have been done for wave-vector transfers in the range 0.75–5.5 times the wave vector at the principal maximum in the static-structure factor, and the theoretical line shapes have been folded with the resolution function for the experiments of Buyers *et al.* Comparison of the position of the maximum, full width at half-maximum, and line shapes with the experimental results gives good agreement.

I. INTRODUCTION

In recent years inelastic-neutron-scattering experiments have provided considerable information on the dynamical behavior of simple liquids. Two systems which have been studied in great detail are the completely quantum case of liquid helium[1] and the essentially classical case of liquid argon.[2] For the case of liquid helium the spectral weight of the density response is all in the frequency region which satisfies the inequality $\hbar\omega \gg k_B T$ (T being the system temperature), whereas the opposite inequality holds for liquid argon. Furthermore, there are additional differences in the two systems relating to the relative magnitude of quantum-mechanical effects. For example, for liquid argon the momentum distribution of the particles is given by the classical Maxwell–Boltzmann function, whereas in liquid helium the momentum distribution is very different and in fact has a singularity due to the quantum-mechanical effect of the Bose–Einstein condensation.

Because the scattering properties of helium and argon are so different, it is of interest to study a system which is in some sense intermediate to them. The only monatomic system in nature which satisfies this requirement is liquid neon. It is a liquid at temperatures between about 25 and 44 °K. The spectral weight for the density response can be concentrated at frequencies either large or small compared to $k_B T/\hbar$, depending on the wavelength of the response being observed. Also there are small but observable quantum-mechanical effects in the structure of liquid neon and specifically on the momentum-distribution function. Buyers, Sears, Lonngi, and Lonngi[3] have performed a neutron-inelastic-scattering experiment on liquid neon, so there are experimental data available with which the theoretical results can be compared. For these reasons there is interest in studying liquid neon.

The theoretical considerations in the present paper are related to those used before for helium and for argon. The zero-temperature limit of this theory was used by Kerr, Pathak, and Singwi[4] for calculations on liquid helium and the high-temperature limit was used by Pathak and Singwi[5] for calculations on liquid argon. In the present paper, the full finite-temperature quantum-mechanical version of the theory will be used.

The outline of this paper is as follows. Section II outlines the theory for the scattering law for liquid neon and particularly discusses the procedure for incorporating the quantum effects in the

momentum-distribution function. Section III contains the results of the calculations and Sec. IV summarizes our conclusions.

II. THEORETICAL FORMULATION

A. Quantum Effects

As was stated in Sec. I, liquid neon is of interest because it is an intermediate case between liquid argon, for which a classical description is adequate, and liquid helium, in which quantum effects are dominant.

The quantum-mechanical effects on the behavior of particles can be classified into two categories.[6] The first of these can be described as essentially a diffraction effect arising from the wave properties of particles; it is important when the de Broglie wavelength of a particle becomes comparable to the particle size. The second effect arises from the requirement that the wave function have the proper symmetry under exchange of identical particles; this effect is important when the de Broglie wavelength becomes comparable to the interparticle spacing. Thus, both effects should be most important for systems of small atomic mass. Further, the diffraction effect is dependent on temperature, becoming more important at low temperature, and the symmetry effect is dependent on both temperature and density, becoming more important at low temperatures and high densities. Also, there is some dependence of the diffraction effect on the density for systems obeying the exclusion principle, since increasing the density at low temperature increases the occupation of higher-energy states; this has the same effect as increasing the temperature.

The de Broglie wavelength of a particle in a many-body system is determined by two different factors. One of these is the scale of the spatial variations of the wave function, which is determined by the Schrödinger equation. The other is the statistical averaging over states which is determined by the temperature.

These effects have been discussed by de Boer in his treatment of the law of corresponding states for the noble gases.[7] If it is assumed that the interparticle potential $V(r)$ can be written in terms of a universal function $f(r)$ as $V(r)=\epsilon f(r/\sigma)$, where the values of the depth parameter ϵ and the range parameter σ depend on the particular system, then the two-particle Schrödinger equation can be written

$$[-(\Lambda/2\pi)^2\nabla^{*2}+f(r^*)]\psi(r^*)=E^*\psi(r^*)\ , \quad (2.1)$$

where r^* is the dimensionless relative coordinate r/σ, ∇^{*2} is the Laplacian with respect to that dimensionless coordinate, and E^* is the dimensionless energy eigenvalue $E^*=E/\epsilon$. The quantity Λ is de Boer's quantum parameter

$$\Lambda=2\pi\hbar/\sigma(M\epsilon)^{1/2}\ , \quad (2.2)$$

where M is the particle mass. From its definition Λ is seen to be the ratio of the de Broglie wavelength to the atomic diameter σ for two particles whose relative energy is ϵ. It is a measure of the competition between the delocalizing effect of the kinetic-energy operator on the energy eigenfunctions and the localizing effect of the attractive part of the potential. For small values of Λ the wave functions are more localized and more nearly classical in behavior, whereas they become more delocalized for larger values of Λ. An equivalent way of saying the same thing is that the zero-point motion is more important for larger Λ.

Since the wave functions give more classical-like behavior in the correspondence limit of high-energy states, and since the statistical weight of these states increases at higher temperatures, the relative importance of these quantum effects is obviously temperature dependent. This dependence can be estimated by introducing the thermal wavelength which, for systems at temperature T that are close to classical behavior, can be defined as

$$\lambda_{th}=2\pi\hbar/(3Mk_BT)^{1/2}, \quad (2.3)$$

where k_B is Boltzmann's constant. λ_{th} is essentially the de Broglie wavelength in a system of temperature T. The natural scale for defining high and low temperature of the system is in units of the well depth ϵ, so that in terms of the reduced temperature $T^*=T/(\epsilon/k_B)$,

$$\lambda_{th}/\sigma=\Lambda/(3T^*)^{1/2}\ . \quad (2.4)$$

Based on the criteria given at the beginning of this section, diffraction effects or the zero-point motion will be more important in systems with larger values of Λ and at low temperatures. Introducing parameters appropriate to neon[8] ($\sigma=2.82$ Å, $\epsilon/k_B=36.3$ °K, and $M=3.32\times10^{-23}$ g) and considering the experimental situation ($T=26.9$ °K and $T^*=0.741$), we have

$$\Lambda_{Ne}=0.574,\quad \lambda_{th}/\sigma=0.39\ . \quad (2.5)$$

For other rare-gas liquids, $\Lambda_{He}=2.68$ and $\Lambda_{Ar}=0.186$. Since the thermal wavelength for neon is about 40% of the atomic size, quantum corrections due to diffraction effects or zero-point motion should contribute a measurable amount to the properties of the system. Exchange effects are much smaller, not only because λ_{th} is a smaller fraction of the interparticle spacing but also because the hard core of the potential reduces them further, as has been shown by Larsen, Kilpatrick, Lieb, and Jordan.[9]

One consequence of the quantum-mechanical zero-point motion is a change in the momentum-distribution function. In classical statistical mechanics

the momentum-distribution function at temperature T of all systems is the Maxwell–Boltzmann function and the average kinetic energy per particle has the value $\frac{3}{2}k_BT$. In quantum statistical mechanics there is no general result for the momentum-distribution function, but it changes in such a way that the average kinetic energy per particle is always greater than the classical value,[10] because of the zero-point motion.

For systems in which the quantum corrections to the classical values are small, these corrections may be obtained by a perturbation calculation in which $\hbar$ is treated as a small quantity. These calculations were first carried out by Wigner[11] and have since been extended by others.[12] The corrections to the free energy of order $\hbar^2$ and $\hbar^4$ have been obtained and also the order $\hbar^2$ correction to the momentum-distribution function.[13]

When corrections to order $\hbar^2$ are incorporated into the momentum-distribution function, it still remains a Gaussian function of the momentum, but the temperature parameter T of the classical formula is replaced by an effective temperature T_{eff} which is greater than T; that is, the number density of particles with momentum $\hbar p$ is

$$n(p) = n\left(\frac{(2\pi\hbar)^2}{2\pi M k_B T_{eff}}\right)^{3/2} e^{-\hbar^2 p^2/2Mk_BT_{eff}} \qquad (2.6)$$

(note that the variable p in this equation is a wave vector), where n is the average number density of the system. The effective temperature is given by[13]

$$T_{eff} = T + \frac{\hbar^2}{12Mk_B^3T^2}\,\frac{1}{3}\,\langle \vec{F}\cdot\vec{F}\rangle_{cl} \ . \qquad (2.7)$$

Here $\vec{F}$ denotes the force on one particle of the liquid owing to the other particles, and $\langle \vec{F}\cdot\vec{F}\rangle_{cl}$ is thus the mean-square force on a single particle. The notation $\langle \ldots \rangle_{cl}$ means that the average is to be taken over the classical phase space of the system.

The quantity appearing in Eq. (2.7) can be written in several alternative ways. Integrating by parts gives

$$\langle \vec{F}\cdot\vec{F}\rangle_{cl} = k_BT\,\langle \nabla_i^2 U\rangle_{cl} \ , \qquad (2.8)$$

where $U(\vec{x}_1, \ldots, \vec{x}_N)$ is the total potential-energy function of the system and ∇_i^2 is the Laplacian with respect to the coordinates of a single particle. If the potential energy is a sum of pairwise interactions, $U = \sum_{i<j} V(\vec{x}_i - \vec{x}_j)$, then

$$\langle \nabla_i^2 U\rangle_{cl} = n\int d\vec{x}\, g_{cl}(x)\,\nabla^2 V(x) \equiv \langle \nabla^2 V\rangle_{cl} \ . \qquad (2.9)$$

Here $g_{cl}(x)$ is the pair-correlation function the system would have if it were completely classical. Presumably, $g_{cl}(x)$ is not very different from the true pair-correlation function $g(x)$ of the liquid. Evaluation of the integral in Eq. (2.9) using an experimental $g(x)$ or a classical $g_{cl}(x)$ from molecular-dynamics calculations thus provides one way of calculating the quantum correction to the momentum distribution.

It should be noted also that the mean-square force on a single particle is related to the fourth frequency moment of the Van Hove self-correlation function.[14]

With $n(p)$ given by Eq. (2.6) the average kinetic energy per particle is $\frac{3}{2}k_BT_{eff}$ and is larger than the classical value as it should be.

The corrections to $n(p)$ which are of higher order than $\hbar^2$ are of two kinds: (i) additional corrections to T_{eff}, which will involve the static correlation functions for three or more particles; (ii) deviations from the Gaussian dependence on p. These higher-order corrections to $n(p)$ are not known, although formulas for $\hbar^4$ corrections to the classical free energy are known.[11,12,15]

This correction to $n(p)$ is the major quantum-mechanical effect which we want to take into account in the theory for the scattering law for liquid neon. This topic is taken up next. A discussion of the magnitude of T_{eff} is given in Sec. III A 1.

B. General Properties of the Scattering Law

The important function used in the theory is the density response function $\chi(q, \omega)$, which gives the proportionality between the amplitude of an applied weak external potential $V^{ext}(\vec{q}, \omega)$ with wave vector $\vec{q}$ and frequency ω and the amplitude of an induced density response $\delta\langle\rho(\vec{q}, \omega)\rangle$:

$$\delta\langle\rho(\vec{q}, \omega)\rangle = \chi(q, \omega)\, V^{ext}(\vec{q}, \omega) \ . \qquad (2.10)$$

The general properties of this function are extensively discussed in the literature[16] and the specific properties of importance for the problem here are discussed in previous papers on similar systems,[4,5,17] so the essential facts will only be listed.

$\chi(q, \omega)$ is a complex-valued function, whose real and imaginary parts, $\chi'(q, \omega)$ and $\chi''(q, \omega)$, respectively, are related by the Kramers–Kronig dispersion relations. The scattering law $S(q, \omega)$ is related to the imaginary part of the density response function by

$$S(q, \omega) = -\frac{\hbar}{\pi n}\,\frac{1}{1 - e^{-\hbar\omega/k_BT}}\,\chi''(q, \omega) \ , \qquad (2.11)$$

which is a specific example of the fluctuation-dissipation theorem. $S(q, \omega)$ is essentially the cross section for the scattering of neutrons with a transfer of momentum $\hbar\vec{q}$ and energy $\hbar\omega$ to the system.[18]

Important quantities associated with $\chi(q, \omega)$ are the low-order frequency moments of its imaginary part. These are[16,19]

$$\frac{-1}{\pi}\int_{-\infty}^{\infty} d\omega\, \chi''(q, \omega)\coth\left(\frac{\hbar\omega}{2k_BT}\right) = \frac{2n}{\hbar}\, S(q) \ , \qquad (2.12)$$

$$\frac{-1}{\pi}\int_{-\infty}^{\infty} d\omega\, \omega\chi''(q,\omega) = \frac{n}{M}\, q^2 \ , \tag{2.13}$$

$$\frac{-1}{\pi}\int_{-\infty}^{\infty} d\omega\, \omega^3\chi''(q,\omega) = \frac{n}{M}\, q^4 \left(2Q_T + \frac{\hbar^2 q^2}{4M} + n\frac{1}{q^2}\int d\vec{x}\, g(x)\,(1-\cos\vec{q}\cdot\vec{x})\,(\hat{q}\cdot\nabla)^2 V(x)\right) \ . \tag{2.14}$$

Here Q_T is the average kinetic energy per particle and $S(q)$ is the static-structure factor, which is related to the pair-correlation function $g(x)$ by the Fourier transformation

$$S(q) - 1 = n\int d\vec{x}\, e^{-i\vec{q}\cdot\vec{x}}[g(x)-1] \ . \tag{2.15}$$

As was explained in detail in Refs. 4 and 5, the theory requires that the approximate expression for the cross section exactly satisfy these low-order-moment relations. They are the coefficients in the short-time expansion of the density response of the system and thus are important in determining the cross section for large momentum and energy transfers.

C. Model Form for $\chi(q,\omega)$

The mean-field model will be used for the density response function. In that model $\chi(q,\omega)$ is assumed to have the form

$$\chi(q,\omega) = \chi_{sc}(q,\omega)/[1-\psi(q)\,\chi_{sc}(q,\omega)] \ . \tag{2.16}$$

The screened response function $\chi_{sc}(q,\omega)$ gives the response of the density to the sum of the external potential and the internal polarization potential, which is related to the function $\psi(q)$ by

$$V_{pol}(q,\omega) = \psi(q)\,\delta\langle\rho(q,\omega)\rangle \ . \tag{2.17}$$

This same form for $\chi(q,\omega)$ has been used previously for calculations on other systems.[4,5,17]

The functions $\chi_{sc}(q,\omega)$ and $\psi(q)$ appearing in Eq. (2.16) must still be determined. To obtain $\chi_{sc}(q,\omega)$ we use the same arguments that were used in Refs. 4 and 5, for liquid helium and liquid argon, respectively. Briefly the argument is that we are interested in obtaining $S(q,\omega)$ for fairly large values of momentum and energy transfer, where the system response should be approaching free-particle-like response. Having introduced the denominator in Eq. (2.16) to allow for the possibility of collective modes, we choose the following form for the imaginary part of the screened response function:

$$\chi''_{sc}(q,\omega) = -\pi\hbar^{-1}\Omega^{-1}\sum_{\vec{p}} n(p)\,[\pi\Gamma(q)]^{-1/2} \times\left[\exp\left(-\frac{(\omega-\omega_{\vec{p}+\vec{q}}+\omega_{\vec{p}})^2}{\Gamma(q)}\right) - \exp\left(-\frac{(\omega+\omega_{\vec{p}+\vec{q}}-\omega_{\vec{p}})^2}{\Gamma(q)}\right)\right] . \tag{2.18}$$

Here Ω is the volume of the system, $\omega_{\vec{p}}$ is the free-particle dispersion relation

$$\omega_{\vec{p}} = \hbar p^2/2M \ , \tag{2.19}$$

and $n(p)$ is the momentum distribution discussed previously. $\Gamma(q)$ is an unknown width function for the Gaussians in Eq. (2.18). If $\Gamma(q)$ is taken to approach zero, then the Gaussians become delta functions and $\chi''_{sc}(q,\omega)$ becomes the imaginary part of the response function for free particles.

The real part of the screened response function is obtained from Eq. (2.18) by using the Kramers–Kronig dispersion relations.

Having made a choice for the form of the screened response function, there are now two unknown functions $\psi(q)$ and $\Gamma(q)$. Because we are interested in the large-q and -ω behavior of the cross section, we require that the density response function describe the short-time behavior of the response exactly. This short-time behavior is given by the moment relations in Eqs. (2.12) to (2.14), so we determine $\psi(q)$ and $\Gamma(q)$ by requiring that these relations be exactly satisfied. The resulting relations are the same as those used by Kerr, Pathak, and Singwi[4] in their calculations for liquid helium.

The first moment relation in Eq. (2.13) is identically satisfied for all $\psi(q)$ and $\Gamma(q)$. Requiring that the third-moment relation in Eq. (2.14) be satisfied gives an equation relating $\psi(q)$ and $\Gamma(q)$, viz.,

$$\frac{3M}{2}\,\frac{\Gamma(q)}{q^2} + n\psi(q) = nP_3(q) \ , \tag{2.20}$$

where

$$P_3(q) = \frac{1}{q^2}\int d\vec{x}\, g(x)\,(1-\cos\vec{q}\cdot\vec{x})\,(\hat{q}\cdot\nabla)^2 V(x) \tag{2.21}$$

is the potential part of the third moment. Now requiring that the zeroth-moment relation [Eq. (2.12)] be satisfied does not give another explicit relation between $\psi(q)$ and $\Gamma(q)$, but must be imposed numerically. [In the high-temperature limit where $\coth(\hbar\omega/2k_BT)$ can be replaced by $(2k_BT/\hbar\omega)$, the integral in Eq. (2.12) can be evaluated using the Kramers–Kronig relations, and two simple formulas for $\psi(q)$ and $\Gamma(q)$ then result. These are the formulas that were used by Pathak and Singwi in their work on liquid argon.[5]]

Having specified $\chi_{sc}(q,\omega)$ and the procedure for obtaining the polarization function $\psi(q)$ and the width function $\Gamma(q)$, the model form for $\chi(q,\omega)$ and $S(q,\omega)$ is now complete.

The final formulas for the scattering law in terms of the functions $\psi(q)$ and $\Gamma(q)$ are as follows: From Eqs. (2.11) and (2.16) the scattering law is

$$S(q,\omega) = -\frac{\hbar}{\pi n}\,\frac{1}{1-e^{-\hbar\omega/k_BT}}$$

$$\times \frac{\chi''_{sc}(q,\omega)}{[1-\psi(q)\chi'_{sc}(q,\omega)]^2+[\psi(q)\chi''_{sc}(q,\omega)]^2} \quad . \quad (2.22)$$

Using the momentum distribution function from Eqs. (2.6) and (2.7) in Eq. (2.18) for $\chi''_{sc}(q,\omega)$ gives

$$\chi''_{sc}(q,\omega) = -\frac{n}{\hbar}\left(\frac{\pi}{W(q)}\right)^{1/2} \times [e^{-(\omega-\omega_q)^2/W(q)} - e^{-(\omega+\omega_q)^2/W(q)}]; \quad (2.23)$$

the Kramers–Kronig transform of this is

$$\chi'_{sc}(q,\omega) = \frac{2n}{\hbar}[W(q)]^{-1/2} \times \left[D\left(\frac{\omega-\omega_q}{[W(q)]^{1/2}}\right) - D\left(\frac{\omega+\omega_q}{[W(q)]^{1/2}}\right)\right]. \quad (2.24)$$

In both Eqs. (2.23) and (2.24) the function $W(q)$ is

$$W(q) = (2k_B T_{eff}/M)q^2 + \Gamma(q) \quad , \quad (2.25)$$

where $\Gamma(q)$ is the function introduced in Eq. (2.18). The function $D(x)$ in Eq. (2.24) is Dawson's integral, defined by

$$D(x) = e^{-x^2}\int_0^x e^{y^2}\,dy \quad . \quad (2.26)$$

For sufficiently large-q values, the scattering law should be described by the impulse approximation,[20,21] in which the interatomic interactions are completely neglected and the distribution of scattered neutrons is given by the Doppler shift of a neutron scattered with momentum transfer $\hbar q$ from a free particle of initial momentum $\hbar p$ averaged over the distribution of initial momenta which are present in the scattering system. Thus

$$\lim_{q\to\infty} S(q,\omega) = S_{IA}(q,\omega) = \sum_{\vec{p}} n(p)\delta(\omega - \omega_{\vec{p}+\vec{q}} + \omega_{\vec{p}}) \quad . \quad (2.27)$$

Using the momentum distribution of Eq. (2.6), this becomes

$$S_{IA}(q,\omega) = \left(\frac{M}{2\pi k_B T_{eff} q^2}\right)^{1/2} \exp\left(\frac{-M(\omega-\omega_q)^2}{2k_B T_{eff} q^2}\right). \quad (2.28)$$

The theory described above reduces to the impulse approximation at sufficiently large q, which can be seen as follows: $P_3(q)$ [defined in Eq. (2.21)] decays as q^{-2} at large q. It was argued in Ref. 4 that $\psi(q)$ must decay to zero more rapidly than q^{-2} and therefore $\Gamma(q)$ must approach a nonzero constant at large q. Equation (2.25) then shows that as q becomes large $\Gamma(q)$ eventually becomes negligible compared to $(2k_B T_{eff}/M)q^2$. In this limit where both $\psi(q)$ and $\Gamma(q)$ can be considered small, this theory reduces to the impulse approximation.

III. CALCULATIONS

The results of the calculations presented here will be compared with the results of the neutron inelastic scattering experiment performed by Buyers *et al.*[3] This experiment was performed at the temperature $T = 26.9\,^{\circ}\mathrm{K}$ and at saturated vapor pressure, which gives a number density $n = 3.66\times10^{-2}$ atoms/Å^3, according to the thermodynamic data of Gibbons.[22]

A neutron diffraction experiment on neon has been carried out by de Graaf and Mozer[23] at $T = 35.05\,^{\circ}\mathrm{K}$ and at three different pressures extending up to 140 atm. However, they have given no data for the inelastic scattering.

A. Auxiliary Quantities

In this subsection the values used for the effective temperature, the static-structure factor, and the integral $P_3(q)$ will be discussed.

1. Effective Temperature

The formula for the effective temperature T_{eff} requires evaluation of either the mean-square force on the particle, as in Eq. (2.7), or the average Laplacian of the interparticle potential using a pair-correlation function for a classical system at the same density and temperature, as in Eq. (2.9).

Molecular-dynamics calculations provide a direct evaluation of the mean-square force, since the force acting on each particle must be obtained to do the calculations, and the average can then be straightforwardly carried out. Verlet[24] has performed such calculations for a system of particles interacting via the Lennard–Jones potential

$$V(r) = 4\epsilon[(\sigma/r)^{12} - (\sigma/r)^6] \quad (3.1)$$

and given values for the quantity

$$\Omega_0^2 = \langle \vec{F}\cdot\vec{F}\rangle_{cl}/Mk_BT \quad (3.2)$$

as a function of the dimensionless density $n^* = n\sigma^3$ and temperature $T^* = T/(\epsilon/k_B)$, where σ and ϵ are the Lennard–Jones parameters. By scaling his results using the parameters appropriate for neon [given just preceding Eq. (2.5)], values for the mean-square force and hence the effective temperature are directly obtained.

In principle there are two advantages in using the the value for the mean-square force obtained in this manner. First, the formula in Eq. (2.7) specifies that the averaging is to be done classically, and that is what is done in the molecular-dynamics calculations. Secondly, this procedure allows one to avoid the problem of evaluating the integral over the classical pair-distribution function in Eq. (2.9). A large contribution to that integral comes from the region close to $x = \sigma$, where the deriva-

tives of the potential are large and where $g(x)$ is rising rapidly from zero and thus most subject to uncertainties. For these reasons we have used the molecular-dynamics value of the mean-square force in evaluating T_{eff}. However, there is the difficulty that the densities and temperatures for which the calculations have been done do not coincide exactly with the temperature and density of the experiment by Buyers *et al.*

Taking Verlet's value of Ω_0^2 at $T=27.6$ °K and $n=3.79\times10^{-2}$ atoms/Å^3 ($T^*=0.76$ and $n^*=0.85$) as closest to the experimental situation gives

$$\frac{\hbar^2}{36Mk_B^3T^2}\langle\vec{\mathrm{F}}\cdot\vec{\mathrm{F}}\rangle_{\mathrm{cl}}=8.37\ ^\circ\mathrm{K},\quad T_{\text{eff}}=35.97\ ^\circ\mathrm{K}\ . \tag{3.3}$$

This quantum correction gives an increase of about 30% in the kinetic energy per particle. This value for T_{eff} has been used in our calculations.

Buyers *et al.* have calculated the quantum corrections at T and n appropriate for the triple point ($T_{\text{tp}}=24.56$ °K and $n_{\text{tp}}=3.62\times10^{-2}$ atoms/Å^3) which is at a somewhat lower temperature and density, by evaluation of the integral in Eq. (2.9), using a classical pair-correlation function also obtained from the molecular-dynamics calculations by Verlet.[25] They obtained

$$\hbar^2\langle\nabla^2V\rangle_{\mathrm{cl}}/36Mk_B^2T=9.82\ ^\circ\mathrm{K}\ , \tag{3.4}$$

which is consistent with Eq. (3.3), since the quantum correction should increase with decreasing temperature.

For purposes of comparison the quantum correction can also be evaluated for the conditions of the de Graaf–Mozer experiment.[23] Taking Verlet's value of Ω_0^2 at $T=38.8$ °K, and $n=3.34\times10^{-2}$ atoms/Å^3 ($T^*=1.069$ and $n^*=0.75$) as being closest to the conditions of that experiment gives

$$\hbar^2\langle\vec{\mathrm{F}}\cdot\vec{\mathrm{F}}\rangle_{\mathrm{cl}}/36Mk_B^3T^2=5.86\ ^\circ\mathrm{K}\ . \tag{3.5}$$

Thus the quantum correction is less important for this experiment.

The form of the $O(\hbar^4)$ correction to $n(p)$ is not known. However, the correction to the free energy of this order for conditions close to the triple point has been calculated by Hansen and Weis[26] and found to be smaller than the $O(\hbar^2)$ correction by a factor of 40. It seems reasonable to assume that the higher-order corrections to $n(p)$ are smaller by the same amount and therefore the $O(\hbar^2)$ correction gives an adequate account of the effects of the zero-point motion on $n(p)$.

2. $P_3(q)$ and $S(q)$

Both $P_3(q)$ and $S(q)$ involve the pair-correlation function $g(x)$, and $P_3(q)$ also requires the potential $V(x)$. The Lennard–Jones potential in Eq. (3.1) was used for $V(x)$. It is then important to have a $g(x)$ which is determined by the same potential, since the main contribution to the integral defining $P_3(q)$ comes from the region around $x=\sigma$, in a similar way to the integral for the mean Laplacian of the potential in Eq. (2.9). Calculations of $P_3(q)$ for liquid He^4 were found to vary as much as 25%, depending on the pair-correlation function used (see the Appendix of Ref. 4). For that reason we chose to use a classical pair-correlation function obtained from the molecular-dynamics calculations of Verlet[25]; among his tabulated functions the closest one to the experimental conditions has $T=29.8$ °K and $n=3.66\times10^{-2}$ atoms/Å^3 ($T^*=0.820$ and $n^*=0.824$). It should be pointed out that Rowe and Sköld[27] have tested the sensitivity of $P_3(q)$ to different pair-correlation functions for liquid argon and found variations of only 2% over the wave-vector range $1.1\le q\le4.4$ Å^{-1}; this is a much smaller variation than was obtained in the liquid-He^4 calculations.

For the special case of the Lennard–Jones potential, the $q=0$ value of $P_3(q)$ is[28] (see the Appendix)

$$nP_3(0)=11p/n+\tfrac{108}{15}Q_T-\tfrac{216}{15}E_T\ , \tag{3.6}$$

where p is the pressure, Q_T is the average kinetic energy per particle, and E_T is the average total energy per particle. Using the values obtained by Verlet[24] for these latter quantities, good agreement is obtained with the value obtained by integrating Eq. (2.21). In principle, Eq. (3.6) could be used to estimate the error in $P_3(0)$ caused by using a classical $g(x)$ instead of a pair-correlation function which includes quantum effects, since formulas are known for the low-order quantum corrections to the classical values of the pressure, kinetic energy, and total energy.[11,12] However, these formulas involve integrations over the three- and four-particle static correlation functions, so that at the present time no reliable estimate of these corrections can be made.

The results for $nP_3(q)/\hbar$ are shown in Fig. 1. It falls rapidly from its $q=0$ value, has some slight oscillations extending out to $q=10$ Å^{-1}, and then decays proportionally to q^{-2} for larger q values.

Having chosen a $g(x)$ to calculate $P_3(q)$, the same $g(x)$ was then transformed according to Eq. (2.15) to obtain $S(q)$. The result is shown in Fig. 2. It is in good agreement with the x-ray diffraction results of Stirpe and Tompson,[29] except for $q\le1.6$ Å^{-1}, where the calculated $S(q)$ shows effects of termination error.

The structure factor for liquid neon is quite similar to that for liquid argon, as measured by Sköld *et al.*[2] and by Yarnell *et al.*,[30] if the q values are scaled according to $q_{\mathrm{Ne}}\sigma_{\mathrm{Ne}}=q_{\mathrm{Ar}}\sigma_{\mathrm{Ar}}$, where σ is the length parameter in the Lennard–Jones potential.

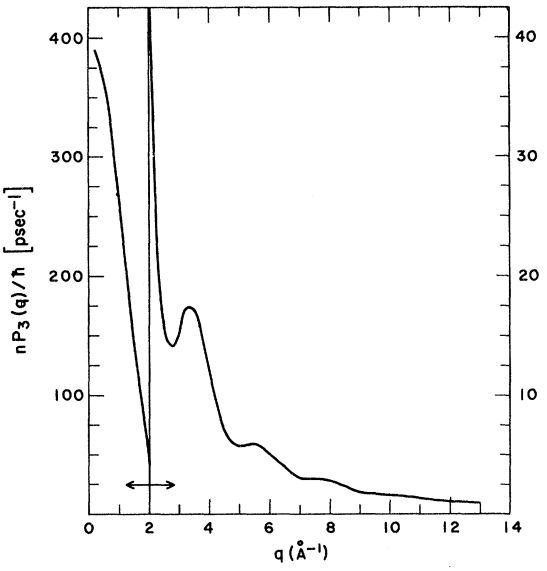

FIG. 1. Potential part of third moment, $nP_3(q)/\hbar$, as defined by Eq. (2.21), vs magnitude of the wave vector q. The integral was evaluated using the pair-correlation function from Ref. 25. (Note that the left-hand scale is to be used for $q \leq 2$ and the right-hand scale for $q > 2$.)

3. Some Calculational Details

Having determined values for all the input functions and parameters, the functions listed at the end of Sec. II were programed and an iterative procedure was set up to integrate $S(q, \omega)$, compare the result with the correct value of $S(q)$, calculate a new $\psi(q)$ and $\Gamma(q)$ always satisfying Eq. (2.20), integrate $S(q, \omega)$ again, and repeat until the correct value for $S(q)$ was obtained. Having obtained $\psi(q)$ and $\Gamma(q)$, line shapes for $S(q, \omega)$, position of its maximum, its maximum value, and its full width at half-maximum were then obtained. Also, we had available the resolution function for the experiments of Buyers *et al.*[3] so we convoluted that with the theoretical $S(q, \omega)$ and obtained quantities which should correspond precisely to what is measured experimentally. These results are described in Sec. III B.

B. Results

$S(q, \omega)$ for liquid neon, considered as a function of frequency for $q \geq 1.8$ Å^{-1}, is a smooth single-maximum curve. The line shapes are slightly asymmetrical, as will be shown further on, but a convenient way to summarize a large amount of data and calculations is to plot the position of the maximum, the full width at half-maximum, and the height of the maximum as functions of q.

In Fig. 3(a) the position of the maximum in $S(q, \omega)$ is plotted, both for the case when the quantum corrections to the momentum-distribution function are taken into account (curve 2) and for the case when these corrections are ignored (curve 3). Also plotted is the free-particle dispersion relation $\omega_q = \hbar q^2/2M$ (curve 1), which is where the maximum of $S(q, \omega)$ is predicted to be by the impulse approximation [cf. Eq. (2.28)]. Experimentally it is easier to locate the points at which $S(q, \omega)$ drops to half of its maximum value than it is to locate the position of the maximum. For this reason Buyers *et al.* have plotted $\omega_{av}(q)$, which is the average of the half-maximum points. Because of the slight asymmetry of the line shapes, $\omega_{av}(q)$ and $\omega_{max}(q)$ do not quite coincide. The experimental and theoretical values for $\omega_{av}(q)$ are shown in Fig. 3(b). The theoretical numbers in both parts of Fig. 3 have *not* been corrected for the effects of the resolution function. Incorporating that causes a very slight shift of $\omega_{max}(q)$ and $\omega_{av}(q)$ to higher frequencies.

These are several things to be noted from the curves in Fig. 3. For $q \lesssim 2.75$ Å^{-1} the maximum in $S(q, \omega)$ is very close to $\omega = 0$ and in that q range most of the spectral weight of $S(q, \omega)$ satisfies the condition $\hbar\omega \ll k_B T$; thus the scattering in this region is very much like that from liquid argon,[2] which is essentially a classical liquid. As q becomes larger than 2.75 Å^{-1}, the maximum shifts to positive values of ω, as is required by detailed balance, and for sufficiently large q it approaches the free-particle recoil value $\omega_q = \hbar q^2/2M$. In this q range the scattering is more like that observed for liquid helium,[1] although the condition $\hbar\omega \gg k_B T$ for most of the spectral weight is satisfied only at the largest q values.

The approach of $\omega_{max}(q)$ to ω_q is not monotonic but oscillatory, which is also like the behavior observed in liquid helium.[1] The minima in $\omega_{max}(q)$ occur at the maxima of the structure factor $S(q)$. This oscillatory behavior is produced in the theory by requiring that the scattering law satisfy the low-order-moment relations. Finally, although both

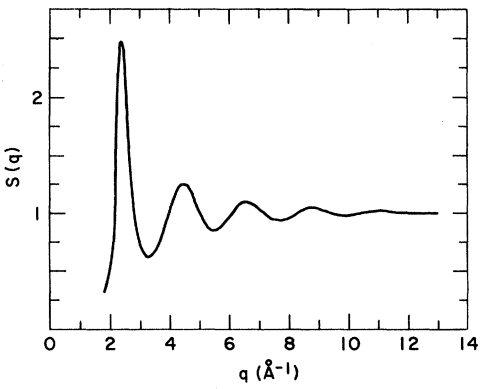

FIG. 2. Static-structure factor $S(q)$ vs q, calculated from the pair-correlation function of Ref. 25.

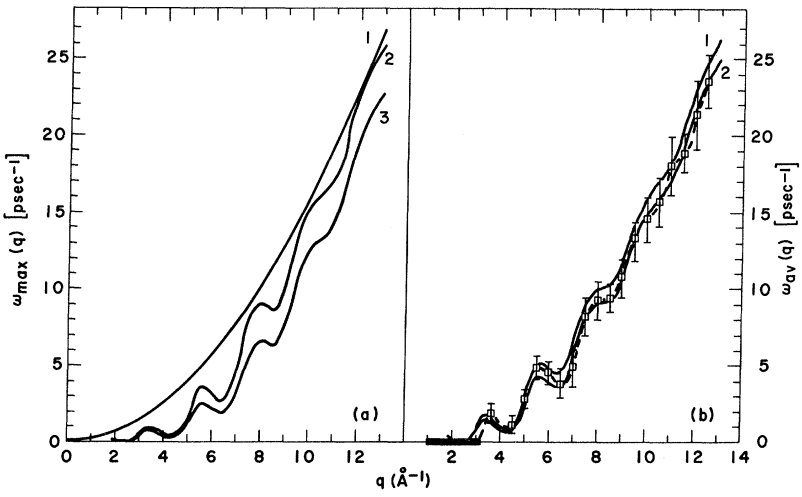

FIG 3. (a) Position of the maximum in $S(q, \omega)$. Curve 1 is the free-particle dispersion curve $\omega_q = \hbar q^2/2M$ and is the position of the maximum in the impulse approximation, Eq. (2.28). Curve 2 is the position of the maximum in the present theory when the quantum correction is *not* taken into account ($T_{\text{eff}} = T$). Curve 3 is the prediction of the present theory when the quantum correction *is* taken into account ($T_{\text{eff}} > T$). (b) Average of the half-maximum points of $S(q, \omega)$. Curve 1 is the result of the present theory when the quantum correction is *not* taken into account ($T_{\text{eff}} = T$). Curve 2 is the result of the present theory when the quantum correction *is* taken into account ($T_{\text{eff}} > T$). The dotted line joins the experimental points which are taken from Ref. 3. For $1.0 \leq q \leq 3.2$ Å^{-1} the experimental maxima are at $\omega = 0$.

curves with and without the quantum correction approach the free-particle recoil curve at large q, it appears that one of the results of the quantum effects is to shift that approach out to larger q values.

The agreement between the theoretical and experimental values for $\omega_{av}(q)$ is good over the whole range of q values. It is somewhat unfortunate that the results both with and without the quantum correction lie within the error bars on the data. It appears that this measurement cannot be used to obtain an accurate value for T_{eff}; however, this is to be expected for this particular quantity since both curves have the same large-q limit. The curve including the quantum correction lies closer to the center of the error bars, except at the smallest q values, so to this extent taking the quantum corrections into account improves the agreement with experiment.

Results for the full width at half-maximum are shown in Fig. 4(a) for four cases. Curves 1 and 2 are the present theory and the impulse approximation, respectively, including the quantum correction; curves 3 and 4 are the same but without the quantum correction. The results in Fig. 4(a) do not include the effects of the resolution function. We have also convoluted our theoretical results for $S(q, \omega)$ with the experimental resolution function for the experiments of Buyers *et al.* and determined the widths of the resulting line shapes. These results are compared with the experimental values in Fig. 4(b).[31] The discontinuities at $q = 4$ and

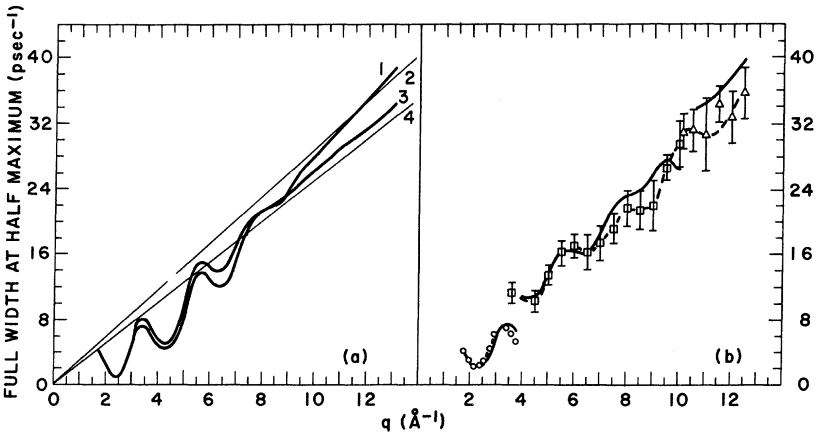

FIG. 4. Full width at half-maximum of $S(q, \omega)$. (a) Curve 1 is the result of the present theory *with* the quantum correction. Curve 2 is the impulse approximation *with* the quantum correction. Curve 3 is the present theory *without* the quantum correction. Curve 4 is the impulse approximation *without* the quantum correction. These curves do *not* include the effect of the resolution corrections. (b) Result of the present theory with the quantum correction and with the experimental resolution function taken into account. The discontinuities are due to changes in the resolution function at those points. The dotted curve joins the experimental points which are from Ref. 3 (also, see Ref. 31). The circles, squares, and triangles are to distinguish among the experimental points taken with different resolution functions.

10 Å^{-1} are due to discontinuities in the resolution function at these points.

The agreement between theory and experiment for the width is good for $q \lesssim 9$ Å^{-1}. For larger q values the calculated width is too large and seems to have less structure than the measured width. Inaccurate input values for $S(q)$ at these large-q values is one possible reason for this discrepancy. The calculated value of $\psi(q)$ in this region is quite sensitive to the deviations of $S(q)$ from unity. Also, as pointed out in Ref. 3, the measured widths are less accurate in this region because the instrumental width is appreciable and the scattered intensity is small.

The width shows oscillations similar to those which have been observed in liquid helium[1] and in liquid argon.[2] These oscillations are also correlated with the oscillations in $S(q)$. Thus these oscillations are the manifestations in a slightly quantum system of the narrowing of $S(q, \omega)$ which was predicted for classical systems by de Gennes many years ago.[32]

It is useful to compare the present calculations with those for liquid argon using the classical limit of this theory.[5,2] In doing so, the values of the wave vector should be scaled according to the prescription $q_{Ar}\sigma_{Ar} = q_{Ne}\sigma_{Ne}$ ($\sigma_{Ar} = 3.41$ Å). In argon the width has maxima at $q_{Ar} = 1$ and 2.78 Å^{-1}, which should scale to $q = 1.21$ and 3.36 Å^{-1} for neon. The first value is below the range of the present calculations, but the second agrees well with the position of the first peak in Fig. 4. However, the theoretical width in argon is about 70% larger than the experimental value at this maximum, whereas in the present neon case the agreement of theory and experiment is much better. It is not understood why this is so.

The present calculations can also be scaled to compare with the liquid-helium results[1,4] using $\sigma_{He} = 2.56$ Å. One would then expect maxima in the width at $q_{He} = 3.7$ and 6.2 Å^{-1}. The *theoretical* results for helium[4] *do not* show maxima at these positions. One reason for this could be that the momentum-distribution function used in those helium calculations, which was obtained from a Jastrow-type wave function by McMillan,[33] is considerably different from the Maxwell–Boltzmann function used here. Another could be that $S(q)$ for liquid helium has considerably less structure than the liquid-neon structure factor. However, it is interesting to note that the *experimental* results for liquid He[4] *do* show maxima at q values which are quite close to those suggested by this simple scaling argument. Since the theory predicts the position of these maxima fairly accurately for both argon and neon, but fails to do so for helium, this causes us to believe that better values of $S(q)$ and $n(p)$ than hitherto available for liquid helium would produce improved agreement in that case also.

The measurement of the width in the asymptotic q region, where the impulse approximation applies, in principle provides a determination of T_{eff}. It can be seen from Eq. (2.28) that in this region the width is a linear function of q with a slope which is proportional to $T_{eff}^{1/2}$. This approach to different straight lines is reasonably evident from Fig. 4(a). However, it can be seen from Fig. 7 that $\Gamma(q)$ has not yet become constant and $\psi(q)$ is not yet zero. Thus even at $q = 13$ Å^{-1} the regime of validity of the impulse approximation has not yet been reached.

The oscillations in the position of the maximum and in the width of $S(q, \omega)$ are now clearly established in liquid neon and in liquid helium both above and below the superfluid transition. They are present in the theory because the approximate formula for the scattering law is required to exactly satisfy the low-order-moment relations, and it is seen from Figs. 1 and 2 that these functions have oscillations extending out to fairly large-q values. These oscillations are a characteristic of dense systems with a strongly repulsive core in the interatomic potential, as has been emphasized by Verlet.[25]

The magnitude of $S(q, \omega)$ at its maximum is shown in Fig. 5, both with and without the resolu-

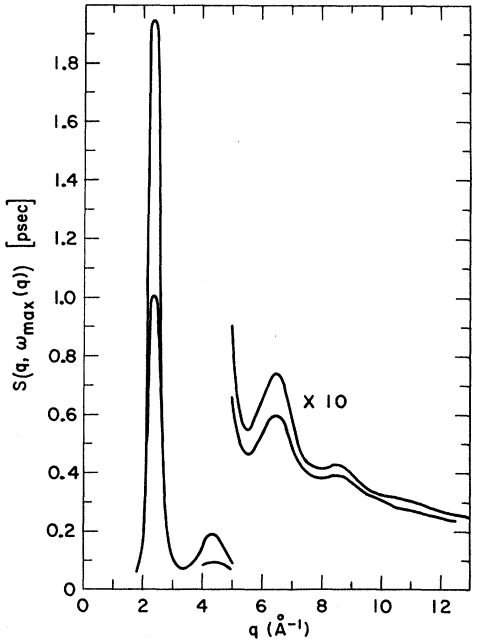

FIG. 5. Maximum value of $S(q, \omega)$, i.e., $S(q, \omega_{max}(q))$. The upper curve does not have resolution corrections. The lower curve does have resolution corrections. The discontinuity in the lower curve at $q = 4$ Å^{-1} is due to a change in the resolution function at that point. The discontinuity in both curves at $q = 5$ Å^{-1} results from multiplying the calculated values by 10 for $q \geq 5$ Å^{-1} in order to display them more clearly.

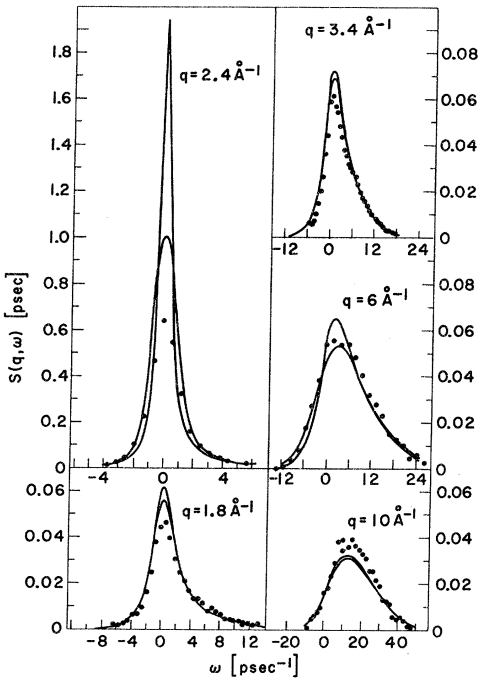

FIG. 6. Line shapes of $S(q, \omega)$ for selected values of q. The curves with the higher maxima do not include the resolution function. The curves with the lower maxima have been corrected for the resolution. The data points are from the experiment of Ref. 3.

tion correction. The position of the four maxima which can be discerned for this function are the same as the positions of the maxima in $S(q)$.

Some selected line shapes are shown in Fig. 6. The curves with the larger maxima have not been corrected for the resolution function, whereas the curves with the lower maxima have been so corrected. The data points are from the experiment of Ref. 3; background corrections have been made on them. The curves of relative intensity from the experiment have been adjusted to the absolute values of the theoretical curves by multiplication with the same constant factor within each of the three ranges of the resolution function (1–3.8, 3.6–10, and 10.0–12.5 Å^{-1}).

The calculated line shapes are generally in good agreement with the data although there are systematic discrepancies. For the smaller values of q the theoretical maxima are too high, whereas at the larger q values the theoretical maxima are too low. A similar situation was found for liquid argon.[2,27] The worst disagreement for the maximum height occurs at $q = 2.4$ Å^{-1}, at the peak of the structure factor. However, the resolution corrections are seen to be large there, so that slight uncertainties in the resolution could produce fairly large uncertainties in the calculated line shape.

Finally, the values of $n\psi(q)/\hbar$ and $[\Gamma(q)]^{1/2}$ are shown in Fig. 7. $\psi(q)$ is negative over the whole q range of interest here, and its magnitude is such that there is no tendency for the first term in the denominator of Eq. (2.22) to vanish. Thus, there are no well-defined collective modes at these q values. It is interesting to note that $\Gamma(q)$, while certainly not constant, has somewhat milder oscillations for liquid neon than were found for liquid argon.[5]

Buyers *et al.*[3] have compared their results with theoretical predictions by Sears.[34,35] For the smaller values of q, Sears's theory uses a memory function approach which gives the correct hydrodynamic limit and also satisfies the same low-order sum rules as the present theory. For the larger values of q, Sears's theory is an expansion of the scattering law in inverse powers of q using a Gram–Charlier series where the coefficients are determined by the same low-order-moment relations. For the position of the maximum, Sears's theory and the present theory agree equally well with the experimental values. For the width, Sears's memory-function approach gives oscillations with the correct period and phase but the magnitudes of the calculated width are too small, whereas the Gram–Charlier expansion gives widths which are too large and have less of an oscillatory character than the experimental results. Thus the results for the width from the present theory are in better agreement with experiment. The other advantage of the present theory is that it covers the whole range of q values used in the experiment.

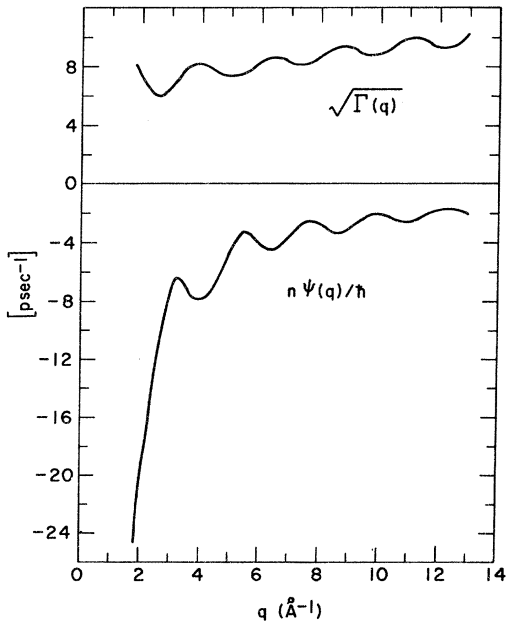

FIG. 7. Width function $\Gamma(q)$ and the polarization potential $\psi(q)$ obtained by satisfying the moment relations.

IV. SUMMARY

The numerical results presented in Sec. III show that the theory used here gives good agreement with the experimental results on liquid neon. The theory is based on three main ideas: (i) assuming a mean-field form for the density response function; (ii) using a nearly free-particle approximation for the screened response function; (iii) requiring exact satisfaction of the low-order-moment relations.

Variations of the present theory have now been applied to several systems[4,5,36] and the conclusion can be reached that this is a useful theory for describing the scattering law for liquids. There are several reasons for this.

The first reason is that minimal outside information is required to be put into the theory, namely, the interparticle potential, the static-structure factor, and the momentum-distribution function. This latter function is just the Maxwell–Boltzmann distribution for a classical system. For the present case it has been found adequate to use the lowest-order quantum correction to the classical distribution. For the quantum case of liquid helium, the momentum distribution must be obtained from some other theory.

The second reason making this a useful theory is that it can be used over the whole range of temperatures from quantum liquids to classical liquids. The detailed balance condition is satisfied, and the quantum-mechanical forms of the moment relations are satisfied when the correct momentum-distribution function is used.

The third reason is that the description of the scattering law given by this theory is in good agreement with experiment for a variety of systems including helium,[4] neon, argon,[5] and sodium.[36] The agreement is not perfect but it is better than is obtained with any other theory which has the same general properties of satisfying the low-order moments, reducing to the impulse approximation at large-q values, and having no adjustable parameters. This has been shown recently in a detailed comparison of several theories with argon-scattering data by Rowe and Sköld.[27]

Since the theory has been applied to a variety of systems, it is useful to compare the results between the different systems, as was done in Sec. III. A significant conclusion resulting from that comparison is that there is need for better values of the momentum-distribution function and the structure factor used in liquid-helium calculations in Ref. 4. Another general result is that the region of validity of the impulse approximation has not been reached for q values as large as 13 Å^{-1}.

Despite its successes, there are several shortcomings of this theory which ought to be clarified. The important formulas of the theory have not been derived from basic considerations. They have rather been based on more intuitive and physical considerations. This is particularly true for the screened response function.

ACKNOWLEDGMENTS

We wish to express our appreciation to Dr. W. J. L. Buyers for very helpful discussions, for making available to us the experimental data, some of them not previously published, which are shown in the figures of this paper, and for giving us the details of the experimental resolution function. One of us (W. C. K.) wishes to express his thanks to Professor J. A. Krumhansl for extending the hospitality of the Laboratory of Atomic and Solid State Physics of Cornell University where some of this work was done, to Dr. J-P. Hansen for very useful conversations, and to Professor H. W. Baird for assistance with the computations.

APPENDIX

The steps leading to Eq. (3.6) will be outlined here. Starting from Eq. (2.21), taking the $q=0$ limit, and carrying out the angular integrations gives

$$P_3(0) = \tfrac{2}{15}\pi \int_0^\infty dx\, x^2 g(x)[3x^2V''(x) + 2xV'(x)] \ . \tag{A1}$$

For the Lennard–Jones potential in Eq. (3.1),

$$3x^2V''(x) + 2xV'(x) = -216\,V(x) - 55xV'(x) \ , \tag{A2}$$

so that

$$nP_3(0) = -\tfrac{22}{3}\pi n \int_0^\infty dx\, x^2 g(x) V'(x) - \tfrac{144}{5}\pi n \int_0^\infty dx\, x^2 g(x) V(x) \ . \tag{A3}$$

These integrals also appear in the virial theorem for the pressure,

$$p = \tfrac{2}{3} nQ_T - \tfrac{2}{3}\pi n^2 \int_0^\infty dx\, x^2 g(x) V'(x) \ , \tag{A4}$$

and the expression for the average energy per particle,

$$E_T = Q_T + 2\pi n \int_0^\infty dx\, x^2 g(x) V(x) \ . \tag{A5}$$

Solving Eqs. (A4) and (A5) for their respective integrals and substituting into Eq. (A3), gives Eq. (3.6).

*Work of one of the authors (W.C.K.) was partially supported by the U.S. Atomic Energy Commission, by the Wake Forest University Faculty Research and Publication Fund, and by the Piedmont University Center; that of the other author (K.S.S.) was

partially supported by the National Science Foundation under Grant No. GP 11054 and by the U.S. Atomic Energy Commission.

[1]R. A. Cowley and A. D. B. Woods, Can. J. Phys. **49,** 177 (1971).

[2]K. Sköld, J. M. Rowe, G. Ostrowski, and P. D. Randolph, Phys. Rev. A **6,** 1107 (1972).

[3]W. J. L. Buyers, V. F. Sears, P. A. Lonngi, and D. A. Lonngi, International Atomic Energy Agency Symposium on Neutron Inelastic Scattering, Grenoble, France, 1972 (unpublished).

[4]W. C. Kerr, K. N. Pathak, and K. S. Singwi, Phys. Rev. A **2,** 2416 (1970); Phys. Rev. A **4,** 2413 (1971).

[5]K. N. Pathak and K. S. Singwi, Phys. Rev. A **2,** 2427 (1970).

[6]J. O. Hirschfelder, C. F. Curtis, and R. B. Bird, *Molecular Theory of Gases and Liquids* (Wiley, New York, 1954); see especially Chap. 6 by J. de Boer and R. B. Bird on the quantum theory and the equation of state.

[7]J. de Boer, Physica (Utr.) 14, 139 (1948).

[8]G. K. Pollack, Rev. Mod. Phys. **36,** 748 (1964).

[9]S. Y. Larsen, J. E. Kilpatrick, E. H. Lieb, and H. F. Jordan, Phys. Rev. 140, A129 (1965).

[10]This can be proven by a trivial application of the Bogoliubov inequality. For one proof of the Bogoliubov inequality and references to other proofs, see, e.g., N. D. Mermin and H. Wagner, Phys. Rev. Lett. **17,** 1133 (1966).

[11]E. Wigner, Phys. Rev. **40,** 749 (1932).

[12]G. Nienhuis, J. Math. Phys. 11, 239 (1970).

[13]L. Landau and I. M. Lifshitz, *Statistical Physics* (Addison-Wesley, Reading, Mass., 1958), p. 102.

[14]B. R. A. Nijboer and A. Rahman, Physica (Utr.) **32,** 415 (1966).

[15]R. N. Hill, J. Math. Phys. 9, 1534 (1968).

[16]D. Pines and P. Nozières, *The Theory of Quantum Liquids* (Benjamin, New York, 1966), Chap. 2.

[17]K. S. Singwi, K. Sköld, and M. P. Tosi, Phys. Rev. A **1,** 454 (1970).

[18]L. Van Hove, Phys. Rev. **95,** 249 (1954).

[19]R. D. Puff, Phys. Rev. 137, A406 (1965).

[20]V. F. Sears, Phys. Rev. **185,** 200 (1969).

[21]H. A. Gersch and P. N. Smith, Phys. Rev. A **4,** 281 (1971).

[22]R. M. Gibbons, Cryogenics **9,** 251 (1969).

[23]L. A. de Graaf and B. Mozer, J. Chem. Phys. **55,** 4967 (1971).

[24]L. Verlet, Phys. Rev. **159,** 98 (1967).

[25]L. Verlet, Phys. Rev. **165,** 201 (1968).

[26]J-P. Hansen and J-J. Weis, Phys. Rev. **188,** 314 (1969).

[27]J. M. Rowe and K. Sköld, International Atomic Energy Agency Symposium on Neutron Inelastic Scattering, Grenoble, 1972 (unpublished).

[28]E. Feenberg, *Theory of Quantum Fluids* (Academic, New York, 1969), p. 91.

[29]D. Stirpe and C. W. Tompson, J. Chem. Phys. **36,** 392 (1962).

[30]J. L. Yarnell, R. G. Wentzel, M. J. Katz, and S. H. Koenig (unpublished).

[31]The experimental results given in Fig. 4(b) of this paper are not quite the same as those presented in Ref. 3. Buyers *et al.* corrected their data for resolution effects by assuming that the natural line shape is Lorentzian and then deconvoluting the resolution function from their data, and it is these corrected results which are presented in Ref. 3. The data shown in Fig. 4(b) are the uncorrected measurements, which were very kindly given to us by Dr. W. J. L. Buyers.

[32]P. G. de Gennes, Physica (Utr.) **25,** 825 (1959).

[33]W. L. McMillan, Phys. Rev. 138, A442 (1965).

[34]V. F. Sears, Can. J. Phys. **48,** 616 (1970).

[35]V. F. Sears, Phys. Rev. **185,** 200 (1969).

[36]K. N. Pathak, K. S. Singwi, G. Cubiotti, and M. P. Tosi, Nuovo Cimento (to be published).